Polarized distribution of inducible nitric oxide synthase regulates activity in intestinal epithelial cells.

Martin Rumbo, Françoise Courjault-Gautier, Frédéric Sierro, Jean-Claude Sirard, Emanuela Felley-Bosco

Polarized distribution of inducible nitric oxide synthase regulates activity in intestinal epithelial cells

Martin Rumbo[2*&], Françoise Courjault-Gautier[1*], Frédéric Sierro[2$], Jean-Pierre Kraehenbuhl[2], Jean-Claude Sirard[2§]and Emanuela Felley-Bosco[1]

[1]Institute of Pharmacology and Toxicology, Rue du Bugnon 27, 1005 Lausanne, Swiss Experimental Cancer Research center, 1066 Epalinges[2] Switzerland

*Martin Rumbo and Françoise Courjault-Gautier contributed equally to the work described

[&] Present address: Departamento de Ciencias Biológicas, Facultad de Ciencias Exactas - Universidad Nacional de La Plata, Argentina

[$] Present address: The Garvan Institute of Medical Research, Darlinghurst, Australia

[§] Present address: Institut de Biologie de Lille, Groupe AVENIR, Equipe Mixte INSERM - Université E0364, Lille, FRANCE

Running title: *Apical iNOS dimer in epithelial cells*

Corresponding author: Emanuela Felley-Bosco, Institute of Pharmacology and Toxicology, Rue du Bugnon 27, 1005 Lausanne, Switzerland, Phone +41 21 6925370, Fax +41 21 6925355, email: emanuela.felley-bosco@ipharm.unil.ch

Abbreviations: DOC, sodium deoxycholate; iNOS, inducible nitric oxide synthase; IFN-γ, interferon-γ; IL-1β interleukin-1β, IL-6, interleukin-6; NO, nitric oxide; TLR5, Toll-like receptor 5; TX-100, Triton X-100

Key words: Inducible nitric oxide synthase; Subcellular distribution; Dimerization; Specific activity, Intestinal epithelial cells

Hal-Inserm Author manuscript

Summary

Inducible nitric oxide synthase (iNOS) functions as a homodimer. In cell extracts, iNOS molecules partition both in cytosolic and particulate fractions, indicating that iNOS exist as soluble and membrane associated forms. In this study, iNOS features were investigated in human intestinal epithelial cells stimulated with cytokines and in duodenum from mice exposed to flagellin. Our experiments indicate that iNOS is mainly associated to the particulate fraction of cell extracts. Confocal microscopy showed a preferential localization of iNOS at the apical pole of intestinal epithelial cells. In particulate fractions, iNOS dimers were more abundant than in the cytosolic fraction. Similar observations were done in mouse duodenum samples. These results suggest that, in epithelial cells, iNOS activity is regulated by localization-dependent processes.

Hal-Inserm Author manuscript

Hal-Inserm Author manuscript

Introduction

The inducible nitric oxide synthase (iNOS) protein is responsible for sustained release of nitric oxide (NO) and is typically synthesized in response to pro-inflammatory stimuli [1]. iNOS protein is induced in a large variety of human diseases, including intestinal disorders such as chronic inflammatory bowel diseases and colon adenocarcinoma [2-4]. The pathobiological function of NO still remains largely uncertain in view of the multiple and even opposite effects of NO. In fact, besides the amount of NO produced, it has been recently suggested that the NO-mediated actions depend on many other factors such as the nature of iNOS induction signal, the cellular and subcellular site of production, subsequent interactions with other cell components and redox environment [5-7]. Although iNOS was originally described as a cytosolic protein [8], it is distributed between cytosol and particulate fraction in activated macrophages [9-11]. It is also present in the particulate but not the cytosolic fraction from guinea-pig skeletal muscle [12] and it localizes in vivo to the apical domain of human bronchial and kidney epithelial cells [13]. iNOS protein is active in a dimeric form [14] but both dimers and monomers can be found in cytoplasm. About 60% of cytosolic iNOS is dimeric in activated murine macrophages [15] and 70% in activated rat hepatocytes [16]. However, nothing is known about dimer-monomer ratio of particulate iNOS. This may be relevant for understanding the control of iNOS and defining targeting strategies for iNOS inhibition. The aim of this study was therefore to characterize iNOS activity both in vitro, using

Hal-Inserm Author manuscript

cytosolic and particulate fraction of activated human intestinal epithelial cells [17], and in vivo, using duodenum samples from mice exposed to bacterial flagellin, which is known to upregulate iNOS expression in intestinal epithelial cells [18].

Experimental procedures

Cell culture

Human intestinal epithelial DLD-1 cells (ATCC CCL-221) were cultured and stimulated with 100 units/ml IFN-γ, 200 units/ml IL-6 (Roche Molecular Biochemicals, Rotkreuz, Switzerland), and 0.5 ng/ml IL-1β (Calbiochem, La Jolla, CA, USA) to induce iNOS as previously described [17]. A stimulation period of 14h was selected from a time course study establishing that iNOS production and activity, which were undetected in control cells, reached maximal levels within 10 hours of cytokine exposure and then remained stable during the following six hours [19].

To investigate iNOS induction in polarized epithelial cells, human intestinal epithelial Caco-2 clone 1 cells, stimulated with cytokines as above were used. Caco-2 cells were grown either on plastic dishes as previously described [20], or on Transwell (6 mm in diameter, 3 μm pore; Corning Costar, Cambridge, MA) where integrity of the epithelial layer was verified by measurement of transepithelial resistance [21].

In some experiments DLD-1 or Caco-2 cells transfected with human iNOS coding cDNA [22] subcloned into the NotI site of the pCIpuro vector, which contains a puromycin resistance gene (kindly provided by

Dr. J. Mirkovitch, Swiss Institute for Experimental Cancer Research, Epalinges, Switzerland) were used.

Mice exposure to flagellin

Protocols involving animals were reviewed and approved by the State Authority (Commission du Service Veterinaire Cantonal, Lausanne, Switzerland). C57BL/6 mice (8–10 weeks old) were challenged (i.v.) with 1 μg of flagellin purified as previously described [21]. Mice were sacrificed after 2h by cervical dislocation and duodenal tissue was processed for RNA and protein analysis as described below.

Cell or tissue lysate preparation and subcellular fractionation

Cell monolayers or 1 cm duodenum tissue were suspended in lysis buffer (50 mM HEPES pH 7.4, 1 mM EGTA, 10% glycerol, 2 μM tetrahydrobiopterin, 2 μM FAD, 5 μg/ml pepstatin, 3 μg/ml aprotinin, 10 μg/ml leupeptin, 0.1 mM 4-(2-aminoethyl)-benzenesulfonyl fluoride, 1 mM sodium vanadate and 50 mM sodium fluoride). Cell samples were then homogenized by three freeze-thaw cycles. Tissues were homogenized using Polytron (Kinematica AG, 6014 Littau, Switzerland). Aliquots of homogenate were centrifuged at 100,000 x g for 15 minutes at 4°C (Beckman Optima TLX Ultracentrifuge). The pellet corresponding to the particulate fraction (48.4±2.7% and 53.8±4.7% of the protein in cultured cells and tissue, respectively) was resuspended by two freeze-thaw cycles in a final volume of lysis buffer equal to the cytosolic. To check cell fractionation, activity of the cytosolic marker lactate dehydrogenase was measured [23] and Western blot analysis of

Na^+, K^+-ATPase, a membrane marker, was performed using a rabbit anti α–subunit antibody (1:20,000) [24].

To further characterize epithelial iNOS, the particulate fraction, was exposed to one of the following treatment: 1) extraction with 1 M KCl, 2) incubation for 1 hour at 4°C with one of the following components prepared in lysis buffer: 0.1 M Na_2CO_3 pH 11; 125 mM NaCl; 1% Triton X-100 (TX-100); 1% TX-100 in the presence of 125 mM NaCl, 3) resuspension in 0.17 M sucrose, 30% glycerol, 10 mM glycine buffer, pH 8.0, containing 0.25% each of sodium deoxycholate (DOC) and Lubrol PX and 1.6 μM $CaCl_2$ and immediate sonication at full power for 10 sec at 4°C [25]. All extracts were separated by centrifugation at 100,000 x g. The supernatant, corresponding to the soluble fraction, was retained and the resulting pellet, corresponding to insoluble material, was resuspended by sonication in the same volume as supernatant.

iNOS activity

Calcium-independent NOS activity was assessed by measuring the conversion of L-[H^3]-arginine to L-[H^3]-citrulline, as previously described [26]. iNOS specific activity was calculated from the ratio of citrulline production to iNOS protein levels.

Western blot analysis

Proteins determination and Western blot analysis were performed as previously described [17,20]. Denatured proteins were separated on 7.5% SDS-polyacrylamide gel. Anti human iNOS antibody (kind gift of Dr. Mumford, Merck Research Laboratories, Rahway, NJ, USA), or anti-murine iNOS (Transduction Laboratories, Lexington, UK) were diluted

Hal-Inserm Author manuscript

at 1:40'000 or 1: 2'000, respectively. Detection was achieved by enhanced chemiluminescence (Amersham Pharmacia, Dubendorf, Switzerland) and densitometry (Imagequant, Molecular Dynamics) was performed on non-saturated films.

Laser dissection microscopy (LMD), RNA isolation and real-time PCR

The gut was rinsed with ice-chilled PBS to remove the intestinal content. One-cm long duodenum segments were cut and villi were microdissected to extract RNA and prepare cDNA as previously described[27]. The latter was amplified by the SYBR-Green PCR assay, and products were detected on a Prism 5700 detection system (SDS, ABI/Perkin-Elmer, Foster City, CA, USA). Beta actin RNA was used to standardize total amount of cDNA. Primers for iNOS (GCTGCCAGGGTCACAACTTT and ACCAGTGACACTGTGTCCCGT) and for beta actin (GCTTCTTTGCAGCTCCTTCGT and CGTCATCCATGGCGAACTG) yielded PCR products of 71 and 59 bp, respectively. Specificity of PCR was checked by analyzing melting curve. Relative mRNA levels were determined by comparing (a) PCR cycle threshold between cDNA of iNOS and beta actin (ΔC), and (b) ΔC values between treated and untreated conditions (ΔΔC) as previously described[7,27].

Immunostaining and confocal microscopy

Caco-2 cells grown on Transwell filters were fixed in PBS 4% paraformaldehyde then permeabilized 5 min with PBS 1% Triton. Immunostaining was carried out by incubation with NO53 anti-iNOS

Hal-Inserm Author manuscript

Hal-Inserm Author manuscript

antibody 1:10'000 followed by revelation using Cy3-conjugated anti-rabbit-immunoglobulin (Ig) G antibodies (Jackson Immunoresearch Laboratories, West Grove, PA) at a dilution of 1/200 for 45 minutes. Filamentous actin expression was detected with Alexa Fluor 488 phalloidin (Molecular probes, Inc, Eugene OR, USA). Caco2 monolayers were analyzed by an LSM-410 Zeiss confocal microscope. XZ sections of monolayers were performed to determine iNOS localization.

Tissue specimens were frozen in OCT embedding compound (Sakura Finetek Europe, Zoeterwoude, The Netherlands) and stored at –80°C. Sections (5-µm thick) were fixed PBS 4% paraformaldehyde then immersed in 0.01 M sodium-citrate buffer (pH 6.0) and placed into a microwave oven for 10 min before incubation with the primary antiserum. Antigen retrieval treatment significantly reduced the strong background obtained in tissue using anti-murine iNOS antibody. Sections were permeabilized 5 min with PBS 0.2% Triton, then sequentially incubated with PBS containing 2% BSA, anti-murine iNOS (overnight at 4°C), followed by revelation using Cy3-conjugated anti-rabbit-immunoglobulin. Since microwave treatment abolishes phalloidin immunoreactivity, phalloidin staining was not performed on tissue sections. For control of unspecific binding of the antibodies, we performed control incubations by applications of isotype matched antibodies directed against different defined antigens. All control experiments were negative. Immunofluorescence was observed with a Zeiss Axiophot immunofluorescence microscope.

Gel filtration chromatography

To determine the relative amounts of iNOS dimers and monomers present in cytosolic and solubilized particulate fraction, size exclusion chromatography was carried out at 4°C using a Sephadex G200 gel filtration column as already described for cytosolic fractions [15,16] or fractions soluble in TX-100 [28]. The column was equilibrated with 40 mM Bis-Tris buffer pH 7.4, containing 2 mM DTT, 10% glycerol and 100 mM NaCl for human iNOS or 200 mM NaCl for murine iNOS [15,16]. Fractions were analyzed for iNOS protein by Western blot. The molecular weights of the protein fractions were estimated relative to gel filtration molecular weigh standards. Gel filtration fractions that fell within a molecular mass range of 600 to 50 kDa (14 fractions) were analyzed by Western blot as described above. The intensity of the iNOS bands were quantitated by densitometry, integrated, and the ratio between monomers and dimers was calculated from these values.

Data analysis

Values are means ± SEM of n independent experiments and statistical analysis was performed using Student's t-test.

Results

Subcellular distribution of iNOS protein and activity in vitro.

The distribution of iNOS protein in the cytosol and particulate fraction was examined in DLD-1 cells exposed to cytokines. To determine the partitioning of iNOS into soluble cytosolic and insoluble membrane-associated forms, cell fractionation was performed. As expected, lactate dehydrogenase activity was recovered at 98±4% (n=4) in the cytosolic fraction, while membrane protein Na^+, K^+-ATPase was

Hal-Inserm Author manuscript

detected only in the particulate fraction (Fig. 1A), indicating that the fractionation procedure is effective. iNOS protein was distributed at 66±2% and 34±2% in the particulate fraction and cytosol, respectively (Fig. 1B and C), leading to a particulate to cytosol ratio of 2.0±0.1. To investigate whether iNOS was delivered as an active enzyme, citrulline production was also determined. Interestingly, compared to iNOS protein ratio, iNOS activity partitioned in higher proportion in particulate vs cytosolic fraction (66±2% versus 19±1%, respectively) (Fig. 1D). In conclusion, iNOS specific activity was 1.8±0.1-fold higher for particulate-bound iNOS than for the cytosolic one ($p<0.001$).

Subcellular distribution of iNOS dimers and monomers

To further characterize iNOS activity, various solubilization protocols as described in material and methods were applied to particulate fractions. As shown in Fig. 2A, complete iNOS protein solubilization was achieved by TX-100/NaCl or Lubrol /DOC. However, TX-100/NaCl reduced iNOS activity by 51±2% (n=3). Solubilization with Lubrol/ was highly effective compared to other methods and resulted in recovery of most iNOS activity (91.1±6.1 %) indicating that this method is more appropriate to solubilize functional iNOS.

The biochemical properties of particulate bound iNOS were independent of cytokine signaling since a similar extraction profile was obtained in DLD-1 cells transfected with human iNOS cDNA (Fig.2B). In transfected cells it was also possible to verify that the same activity was recovered when cells were harvested either in lysis buffer or in

Hal-Inserm Author manuscript

Lubrol/DOC (data not shown), indicating that treatment with these detergent does not result in artificial increase of iNOS activity.

Taken together these data indicate that in epithelial intestinal cells iNOS intrinsically associates with particulate matter and intact activity can be extracted with Lubrol/DOC.

Since iNOS activity requires dimerization[14], we investigated iNOS oligomerisation in cell fractions using gel filtration chromatography, which allows defining the amount of monomers and dimers. Western blot analysis of chromatography fractions showed that only dimers were present in the particulate compartment (Fig.3). In contrast, some cytosolic iNOS is in monomeric form (monomers/ dimers estimated to 0.33±0.06, n=3). Using this information it is possible to calculate how much of the protein present in the cytosol (Fig.1) is under dimeric form. Indeed total protein in this compartment is represented by the sum of monomer plus dimer. Knowing that monomer=0.33*dimer, total iNOS protein is equivalent to 1.33*dimer. Therefore, the level of dimer was estimated to 26% (34%/1.33) of total iNOS in cytosol whereas it reached 100% in particulate fraction. Thus, iNOS specific activity standardized to iNOS dimer levels was not significantly different in particulate-associated and cytosolic iNOS. In conclusion, these results suggest that the prevalence of iNOS dimers is essential for enrichement in iNOS activity within the particulate fraction of epithelial cells.

Apical distribution of iNOS in intestinal epithelial cells

Hal-Inserm Author manuscript

To get more insight into the localization of iNOS in intestinal cells, Caco-2 cells were investigated. CaCo-2 cells spontaneously differentiate to enterocyte-like cells when they are cultured for 20 days after confluency onto plastic or for 10 days on filters. At this stage they form polarized monolayers sealed by tight junctions, and display a well-developed apical brush border membrane expressing specific enterocyte hydrolases [29]. As previously described [20], iNOS protein decreased upon differentiation in CaCo-2 cells (Fig.4A left panel). After cytokine addition, iNOS expression was dramatically increased in Caco-2 cells in both proliferating and differentiated cells (Fig.4A left panel). iNOS was also expressed after CaCo-2 transfection with human iNOS cDNA (Fig.4A right panel). As in DLD-1 cells, iNOS was mostly associated to particulate matter in cytokine-activated or iNOS-transfected cells (data not shown). To correlate the iNOS partitioning in particulate fraction to a specific subcellular distribution, immunostaining was performed on differentiated enterocyte (Fig.4B). Confocal microscopy showed that iNOS localized to the apical domain of enterocytes and co-localized with filamentous actin (Fig. 4B left panel). The apical distribution was independent of cytokine stimulation as assessed with Caco-2 cells transfected with human iNOS cDNA (Fig.4B, right lower panel).

Taken together, these data suggest a specific localization of iNOS to apical domains of intestinal epithelial cells.

Particulate fraction association of iNOS in vivo

In order to determine the distribution of iNOS in intestinal epithelial cells *in vivo*, experiments were conducted in mice injected with bacterial flagellin. Flagellin activates TLR5, which induces iNOS expression in intestinal epithelial cells in vivo [18]. Quantitative RT-PCR showed 5-fold induction of iNOS mRNA levels in duodenum of flagellin-treated compared to untreated animals (Fig.5A). We also found a 50-fold induction of iNOS mRNA levels in microdissected epithelium from villi (Fig.5A) which indicates that epithelial cells were the main source of iNOS. In addition, production of iNOS protein was significantly uupregulated in mice exposed to flagellin (Fig.5B). Immunostaining of duodenum sections revealed that iNOS was distributed apically in intestinal crypts (Fig. 6A) corroborating observation in cultured polarized cells. Soluble and particulate fractions were extracted from intestinal homogenate from flagellin exposed mice and analyzed by Western blot (Fig. 6B, left panel). We found that iNOS protein was 4.6 fold more abundant into the particulate fraction than into the cytosol. iNOS activity was distributed 87±12% in the particulate fraction and 13±12% in the cytosolic fraction (Fig. 6B, right panel). Thus, iNOS activity normalized by total iNOS protein was 1.5-fold higher for particulate-bound iNOS than for the cytosolic ($p<0.05$).

The iNOS monomers/ dimers ratio was 0.60±0.08 (n=3) for cytosolic fraction and 0.20±0.04 (n=3) for the particulate fraction. These results indicate that iNOS dimer in flagellin-stimulated intestine corresponded to 11% and 69% in cytosol and particulate fraction, respectively. Therefore,

Hal-Inserm Author manuscript

Hal-Inserm Author manuscript

the preferential partioning of iNOS activity into particulate fraction likely results from the enrichement in iNOS dimers.

Discussion

While the occurrence of iNOS in particulate cellular fraction is known for several years [9-11,13], the biological significance of this association is not clear at the moment. Our results showed that both, in vitro and in vivo, most iNOS protein or activity is associated to the particulate fraction in intestinal epithelial cells. These results are consistent with iNOS features in neutrophils from urine of patients with bacterial urinary tract infection [30], primary proximal tubule, human bronchial epithelial cells 16HBE14o- [13] and activated rodent macrophages [9-11,28]. Previous studies have shown that iNOS interacts with cytoskeleton via components like α-actinin 4 [28] and proteins harboring spectrin-like motif [31]. We found that epithelial iNOS co-localized also with actin cytoskeleton proteins. A recent study shows that the C-terminus of iNOS promotes in vitro interactions with the PDZ protein EBP50 [13]. Interestingly, EBP50 has different binding partners including ezrin that can be anchored to the actin cytoskeleton [32].

Our solubilization protocol allows efficient recovery of iNOS activity and analysis of monomer/dimer ratio in particulate fractions [14-16,33]. Previous investigations focused on cytosolic fractions or fractions soluble in 0.1% TX-100 [28], which do not represent total iNOS [10]. Our data show that iNOS activity in epithelial cells is not only controlled by the number of iNOS molecules but also by the oligomerisation feature in subcellular fractions. Variation in iNOS specific activity was correlated

to subcellular localization. In murine macrophages, co-expression of Rac2, a member of the Rho GTPase family, led to a specific distribution of iNOS to insoluble fraction. Furthermore, iNOS activity increases without change in protein levels [34]. Similarly, inhibitiontion of iNOS interaction with the α-actinin 4 results in loss of activity [28].

Targeting iNOS activity to specific cellular domain is independent of stimulation since a similar distribution is observed in transfected cells. Taken together these observations indicate that cells set up efficient strategies to bring iNOS where NO production is required. This may be necessary, as proposed by others[35], to direct NO toward extracellular pathogens, which, in intestinal cells, could be bacteria present in the intestinal lumen. This hypothesis is supported by positioning of iNOS on the apical side of intestinal crypts. Recently PDZ-binding α_2/β_1-NO-sensitive guanylate-cyclase[36] was found to be expressed in intestinal tissue[37]. Active iNOS might be targeted to this NO-sensitive form of guanylate cyclase via PDZ-dependent mechanisms. Nitric oxide can also interact with superoxide to form the strong oxidant peroxynitrite[38,39]. Superoxide is produced in vivo by membrane-associated NADPH oxidase complex, which is present in intestinal epithelial cells[40-42]. Exposure of NADPH oxidase expressing-human intestinal cells to flagellin can increase superoxide production[42]. Combined with our observation that flagellin increases expression of a particulate fraction-associated iNOS, this suggests a co-localization and a functional synergy between these enzymes.

Hal-Inserm Author manuscript

Hal-Inserm Author manuscript

Different scenarios can be considered according to the iNOS dimer enrichment in the particulate fraction. One possibility is that the scaffolding protein anchoring iNOS to the particulate fraction recognizes mainly the active dimer. This might explain why under denaturing conditions iNOS did not immunoprecipitate with PDZ protein EBP50 [13]. Alternatively, monomers might have distinct turnover rate depending on their subcellular localization. The fact that antifungal molecule clotrimazole is able to change the ratio of dimeric to monomeric iNOS in the cytosol without affecting total protein amount [33,43] favors the hypothesis that iNOS monomers are stable in the cytosol. On the other hand we have shown that proteasomal iNOS degradation seems to occur in detergent insoluble domains [17].

In conclusion, this study in cytokine- or flagellin- stimulated intestinal epithelial cells corroborated previous observations of iNOS accumulation in the particulate cellular fraction and showed for the first time that monomeric to dimeric iNOS ratio is different in particulate versus cytosolic fraction. These results indicate a new regulation of iNOS activity relying on localization-dependent molecular conformation and provide tools for further investigation of the mechanisms involved in this differential iNOS distribution.

Acknowledgments

We thank Jérôme Dall'Aglio and Sébastien Brunetti for their skillful assistance and Dr Michèle Markert for helpful discussion. This work was

supported by the Swiss National Science Foundation (SNSF 3100A0-103928) and EC grant QLRT2001-02357.

References

1. MacMicking J., Xie Q. W., and Nathan C. (1997) Nitric oxide and macrophage function. *Annu.Rev.Immunol* **15**, 323-350.

2. Kroncke K. D., Fehsel K., and Kolb-Bachofen V. (1998) Inducible nitric oxide synthase in human diseases. *Clin.Exp.Immunol.* **113**, 147-156.

3. Ambs S., Merriam W. G., Bennett W. P., Felley-Bosco E., Ogunfusika M. O., Oser S. M., Klein S., Shields P. G., Billiar T. R., and Harris C. C. (1998) Frequent nitric oxide synthase-2 expression in human colon adenomas: implication for tumor angiogenesis and colon cancer progression. *Cancer Res.* **58**, 334-341.

4. Singer I. I., Kawka D. W., Scott S., Weidner J. R., Mumford R. A., Riehl T. E., and Stenson W. F. (1996) Expression of inducible nitric oxide synthase and nitrotyrosine in colonic epithelium in inflammatory bowel disease. *Gastroenterology* **111**, 871-885.

Hal-Inserm Author manuscript

5. Espey M. G., Miranda K. M., Pluta R. M., and Wink D. A. (2000) Nitrosative capacity of macrophages is dependent on nitric-oxide synthase induction signals. *J.Biol.Chem.* **275**, 11341-11347.

6. Miller M. J. S. and Sandoval M. (1999) Nitric Oxide III. A molecular prelude to intestinal inflammation. *Am.J.Physiol.* **276**, G795-G799.

7. Andre M. and Felley-Bosco E. (2003) Heme oxygenase-1 induction by endogenous nitric oxide: influence of intracellular glutathione. *FEBS. Lett.* **546**(2-3), 223-227.

8. Moncada S., Palmer R. M. J., and Higgs E. A. (1991) Nitric oxide: physiology, pathophysiology, and pharmacology. *Pharmacol.Rev.* **43**, 109-142.

9. Schmidt H. H. H. W., Warner T. D., Nakane M., Fostermann U., and Murad F. (1992) Regulation and subcellular location of nitrogen oxide synthases in RAW264.7 macrophages. *Mol.Pharmacol.* **41**, 615-624.

10. Vodovotz Y., Russell D., Xie Q., Bogdan C., and Nathan C. (1995) Vesicle membrane association of nitric oxide synthase in primary mouse macrophages. *J.Immunol.* **154**, 2914-2925.

Hal-Inserm Author manuscript

11. Webb J. L., Harvey M. W., Holden D. W., and Evans T. J. (2001) Macrophage nitric oxide synthase associates with cortical actin but is not recruited to phagosomes. *Infect. Immun.* **69**(10), 6391-6400.

12. Gath I., Closs E. I., Gödtel-Armbrust U., Smitt S., Nakane M., Wessler I., and Förstermann U. (1996) Inducible NO synthase II and neuronal NO synthase I are constitutively expressed in different structures of guinea pig skeletal muscle: implications for contractile function. *Faseb J.* **10**, 1614-1620.

13. Glynne P. A., Darling K. E., Picot J., and Evans T. J. (2002) Epithelial inducible nitric oxide synthase is an apical EBP50-binding protein that directs vectorial nitric oxide output. *J.Biol.Chem.* **277**, 33132-33138.

14. Baek K. J., Thiel B. A., Lucas S., And Stuehr D. J. (1993) Macrophage Nitric Oxide Synthase Subunits. *J.Biol.Chem.* **268**, 21120-21129.

15. Albakri Q. A. and Stuehr D. J. (1996) Intracellular assembly of inducible NO synthase is limited by nitric oxide-mediated changes in heme insertion and availability. *J.Biol.Chem.* **271**, 5414-5421.

Hal-Inserm Author manuscript

16. Park J. H., Na H. J., Kwon Y. G., Ha K. S., Lee S. J., Kim C. K., Lee K. S., Yoneyama T., Hatakeyama K., Kim P. K., Billiar T. R., and Kim Y. M. (2002) Nitric Oxide (NO) Pretreatment Increases Cytokine-induced NO Production in Cultured Rat Hepatocytes by Suppressing GTP Cyclohydrolase I Feedback Inhibitory Protein Level and Promoting Inducible NO Synthase Dimerization. *J.Biol.Chem.* **277**(49), 47073-47079.

17. Felley-Bosco E., Bender F. C., Courjault-Gautier F., Bron C., and Quest A. F. G. (2000) Caveolin-1 down-regulates inducible nitric oxide synthase via the proteasome pathway in human colon carcinoma cells. *Proc. Natl. Acad. Sci. USA* **97**, 14334-14339.

18. Eaves-Pyles T., Murthy K., Liaudet L., Virag L., Ross G., Soriano F. G., Szabo C., and Salzman A. L. (2001) Flagellin, a novel mediator of Salmonella-induced epithelial activation and systemic inflammation: I kappa B alpha degradation, induction of nitric oxide synthase, induction of proinflammatory mediators, and cardiovascular dysfunction. *J.Immunol.* **166**(2), 1248-1260.

19. Courjault-Gautier F., Aurora A., and Felley-Bosco E. (2000) Induction time-course and subcellular distribution of the human inducible nitric oxide synthase in an intestinal cell line: evidence for post-translational regulation. In *The biology of nitric oxide.*

Hal-Inserm Author manuscript

Part 7, (eds. Moncada S., Gustafsson L. E., Wiklund N. P., and Higgs E. A.), p. 155. Portland Press, London.

20. Vecchini F., Pringault E., Billiar T. R., Geller D. A., Hausel P., and Felley-Bosco E. (1997) Decreased activity of inducible nitric oxide synthase type 2 and modulation of the expression of glutathione S-transferase alpha, bcl-2, and metallothioneins during the differentiation of CaCo-2 cells. *Cell Growth Differ.* **8**, 261-268.

21. Sierro F., Dubois B., Coste A., Kaiserlian D., Kraehenbuhl J. P., and Sirard J. C. (2001) Flagellin stimulation of intestinal epithelial cells triggers CCL20-mediated migration of dendritic cells. *Proc. Natl. Acad. Sci. U. S. A.* **98**(24), 13722-13727.

22. Geller D. A., Lowenstein C. J., Shapiro R. A., Nussler A. K., Di Silvio M., Wang S. C., Nakayama D. K., Simmons R. L., Snyder S. H., and Billiar T. R. (1993) Molecular cloning and expression of inducible nitric oxide synthase from human hepatocytes. *Proc. Natl. Acad. Sci. USA* **90**, 3491-3495.

23. Bermeyer H. U. and Bernt E. (1974) Lactate deshydrogenase UV-assay with pyruvate and NADH. In *Methods of enzymatic analysis*, (ed. Bermeyer H. U.), pp. 574-579. Academic Press, New York.

Hal-Inserm Author manuscript

24. Féraille E., Carranza M. L., Gonin S., Béguin P., Pedemonte C., Rousselot M., Caverzasio J., Geering K., Martin P.-Y., and Favre H. (1999) Insulin-induced stimulation of Na+,K+-ATPase activity in kidney proximal tubule cells depends on phosphorylation of the æ-subunit at Tyr-10. *Mol.Biol.Cell* **10**, 2847-2859.

25. Glass G. A., DeLisle D. M., DeTogni P., Gabig T. G., Magee B. H., Markert M., and Babior B. M. (1986) The respiratory burst oxidase of human neutrophils. Further studies of the purified enzyme. *J.Biol.Chem.* **261**(28), 13247-13251.

26. Felley-Bosco E., Ambs S., Lowenstein C. J., Keefer L. K., and Harris C. C. (1994) Constitutive expression of inducible nitric oxide synthase in human bronchial epithelial cells induces c-fos and stimulates the cGMP pathway. *Am.J.Respir.Cell Mol.Biol.* **11**, 159-164.

27. Rumbo M., Sierro F., Debard N., Kraehenbuhl J.-P., and Finke D. (2004) Lymphotoxin â receptor signaling induces the chemokine CCL20 in intestinal epithelium. *Gastroenterology* **in press**.

28. Daniliuc S., Bitterman H., Rahat M. A., Kinarty A., Rosenzweig D., and Nitza L. (2003) Hypoxia inactivates inducible nitric oxide

Hal-Inserm Author manuscript

synthase in mouse macrophages by disrupting its interaction with alpha-actinin 4. *J.Immunol.* **171**(6), 3225-3232.

29. Zweibaum A., Laburthe M., Grasset E., and Louvard D. (1991) Use of cultured cell lines in studies of intestinal cell differentiation and function. In *Handbook of Physiology*, (eds. Field M. and Frizzell R. A.), pp. 223-255. American Physiology Society, Bethesda.

30. Wheeler M. A., Smith S. D., Garcia-Cardena G., Nathan C. F., Weiss R. M., and Sessa W. C. (1997) Bacterial infection induces nitric oxide synthase in human neutrophils. *J.Clin.Invest.* **99**, 110-116.

31. Ratovitski E. A., Alam M. R., Quick R. A., McMillan A., Bao C., Kozlovsy C., Hand T. A., Johnson R. C., Mains R. E., Eipper B. A., and Lowenstein C. J. (1999) Kalirin inhibition of inducible nitric-oxide synthase. *J.Biol.Chem.* **274**, 993-999.

32. Shenolikar S. and Weinman E. J. (2001) NHERF: targeting and trafficking membrane proteins. *Am. J. Physiol. Renal. Physiol.* **280**(3), F389-F395.

33. Sennequier N., Wolan D., and Stuehr D. J. (1999) Antifungal imidazoles block assembly of inducible NO synthase into an active dimer. *J.Biol.Chem.* **274**(2), 930-938.

34. Kuncewicz T., Balakrishnan P., Snuggs M. B., and Kone B. C. (2001) Specific association of nitric oxide synthase-2 with Rac isoforms in activated murine macrophages. *Am.J.Physiol.* **281**, f326-336.

35. Darling K. E. A. and Evans T. J. (2003) Effects of nitric oxide on Pseudomonas aeruginosa infection of epithelial cells from a human respiratory cell line derived from a patient with cystic fibrosis. *Infect. Immun.* **71**(5), 2341-2349.

36. Russwurm M., Wittau N., and Koesling D. (2001) Guanylyl Cyclase/PSD-95 Interaction. targeting of the nitric oxide-sensitive alpha 2beta 1 guanylyl cyclase to synaptic membranes. *J.Biol.Chem.* **276**(48), 44647-44652.

37. Mergia E., Russwurm M., Zoidl G., and Koesling D. (2003) Major occurrence of the new alpha(2)beta(1) isoform of NO-sensitive guanylyl cyclase in brain. *Cell. Signal.* **15**(2), 189-195.

38. Huie R. E. and Padmaja S. (1993) The reaction of NO with superoxide. *Free Radical Research Communications* **18**, 195-199.

Hal-Inserm Author manuscript

39. Beckman J. S. and Koppenol W. H. (1996) Nitric oxide, superoxide, and peroxynitrite: the good, the bad, and the ugly. *Am.J.Physiol.* **271**, C1424-C1437.

40. Suh Y.-A., Arnold R. S., Lassegue B., Shi J., Xu X., Sorescu D., Chung A. B., Griendin K. K., and Lambeth J. D. (1999) Cell transformation by the superoxide-generating oxidase Mox1. *Nature* **401**, 79-82.

41. Banfi B., Maturana A., Jaconi S., Arnaudeau S., Laforge T., Sinha B., Ligeti E., Demaurex N., and Krause K.-H. (2000) A mammalian H+ channel generated through alternative splicing of the NADPH oxidase homolog NOH-1. *Science* **287**, 138-142.

42. Kawahara T., Kuwano Y., Teshima-Kondo S., Takeya R., Sumimoto H., Kishi K., Tsunawaki S., Hirayama T., and Rokutan K. (2004) Role of nicotinamide adenine dinucleotide phosphate oxidase 1 in oxidative burst response to toll-like receptor 5 signaling in large intestinal epithelial cells. *J.Immunol.* **172**(5), 3051-3058.

43. Kuo P. C. and Abe K. Y. (1995) Cytokine-mediated production of nitric oxide in isolated rat hepatocytes is dependent on cytochrome P-450III activity. *FEBS. Lett.* **360**(1), 10-14.

Hal-Inserm Author manuscript

Figure Legends

FIG. 1. Subcellular distribution of iNOS in human cultured intestinal cells. DLD-1 cells were incubated with cytokines for 14 hours before cell fractionation. A, distribution of Na^+, K^+-ATPase or LDH in cytosol (C) and particulate (P) fractions. B, Subcellular distribution of iNOS protein. Equal volumes of the cytosolic and particulate were analyzed. C, densitometric analysis of iNOS protein distribution. The protein amount in each fraction was expressed relatively to the iNOS amount found in homogenate and values are the means ± SEM from 7 independent experiments. D, Subcellular distribution of iNOS activity. The enzyme activity was determined by the amount of citrulline produced in cytosol versus resuspended particulate fraction and was expressed as % of the production measured in the whole cell homogenate (64.3±6.3 pmol/min.mg protein n=7). Values are the means ± SEM from 7 independent experiments.

FIG. 2. Effect of salts and detergents on iNOS association with membranes in cultured cells. A. Particulate fractions prepared from cytokine-treated cells were extracted with 1M KCl or incubated for 1 hour with one of the following components prepared in lysis buffer: 0.1M Na_2CO_3 pH 11; 125 mM NaCl; 1% TX-100; 1% TX-100 together with 125 mM NaCl or sonicated after addition of Lubrol-DOC. Soluble (S) and insoluble (I) material were separated by centrifugation at 100'000g. The insoluble pellet was resuspended by sonication in the

Hal-Inserm Author manuscript

same volume as supernatant and equal volumes of the two fractions were loaded. B. DLD-1 cells transfected with iNOS were incubated for 1 hour with one of the following components prepared in lysis buffer: 125 mM NaCl; 1% TX-100; 1% TX-100 together with 125 mM NaCl or sonicated after addition of Lubrol-DOC. Soluble (S) and insoluble (I) material were separated by centrifugation at 100'000g. The insoluble pellet was resuspended by sonication in the same volume as supernatant and equal volumes of the two fractions were loaded. Blot shown is representative of 3 independent experiments.

FIG. 3. Distribution of iNOS monomers and dimers in solubilized particulate fraction (P) and cytosol (C) of DLD-1 cells stimulated during 14h with cytokines. Lubrol-DOC extracts of particulate fraction and cytosols were fractionated by gel filtration chromatography and column fractions were analyzed by SDS-PAGE and Western blot. Fractions were designated to contain iNOS dimers or monomers based on the estimated molecular weight of the gel filtration fraction. Blot shown is representative of 3 independent experiments.

FIG. 4. iNOS localizes to the apical domain of polarized intestinal epithelial cells. A. Western blot analysis of iNOS expression 15h after cytokine stimulation of proliferative vs differentiated cells (left panel) or in Caco-2 cells transfected with iNOS (right panel). Actin was used as control for protein loading. B. xz confocal sections of cytokine treated CaCo-2 cells (left panel) or iNOS transfected CaCo-2 cells (bottom right

Hal-Inserm Author manuscript

panel, not all transfected cells expressed iNOS). Cells were immunostained using anti -iNOS and phalloidine (F-actin detection). Only F-actin staining was observed when sections from cells exposed to cytokine15h were stained without the iNOS primary antibody (control: upper right panel). The arrows indicate the position of the filter (basolateral side of cells). Scale bar = 6 μm.

FIG. 5. Expression of iNOS in duodenum tissue of mice. A. Quantification of iNOS mRNA induction by flagellin in whole tissue and microdissected villi assessed by real-time PCR. B. Western blot analysis of iNOS protein expression in control or flagellin exposed mice. Actin was used as control for protein loading.

Fig. 6. Subcellular distribution of iNOS in murine duodenum tissue.

A. Duodenum sections of flagellin exposed or control mice were immunostained using anti-iNOS antibody. Each condition is representative of three mice. Scale bar = 40 μm. B. Homogenate (H), cytosolic (C), Lubrol/DOC extracted particulate fractions (S) and insoluble pellet (I) were analyzed by Western blot (left panel). Densitometric analysis of iNOS protein and distribution of iNOS activity in cytosol vs Lubrol/DOC extracts (right panel). Whole duodenum homogenate activity amounted to 32±14 pmol citrulline/min.mg prot (n=4). Values are the means ± SEM from 4 independent experiments.

Hal-Inserm Author manuscript

Hal-Inserm Author manuscript

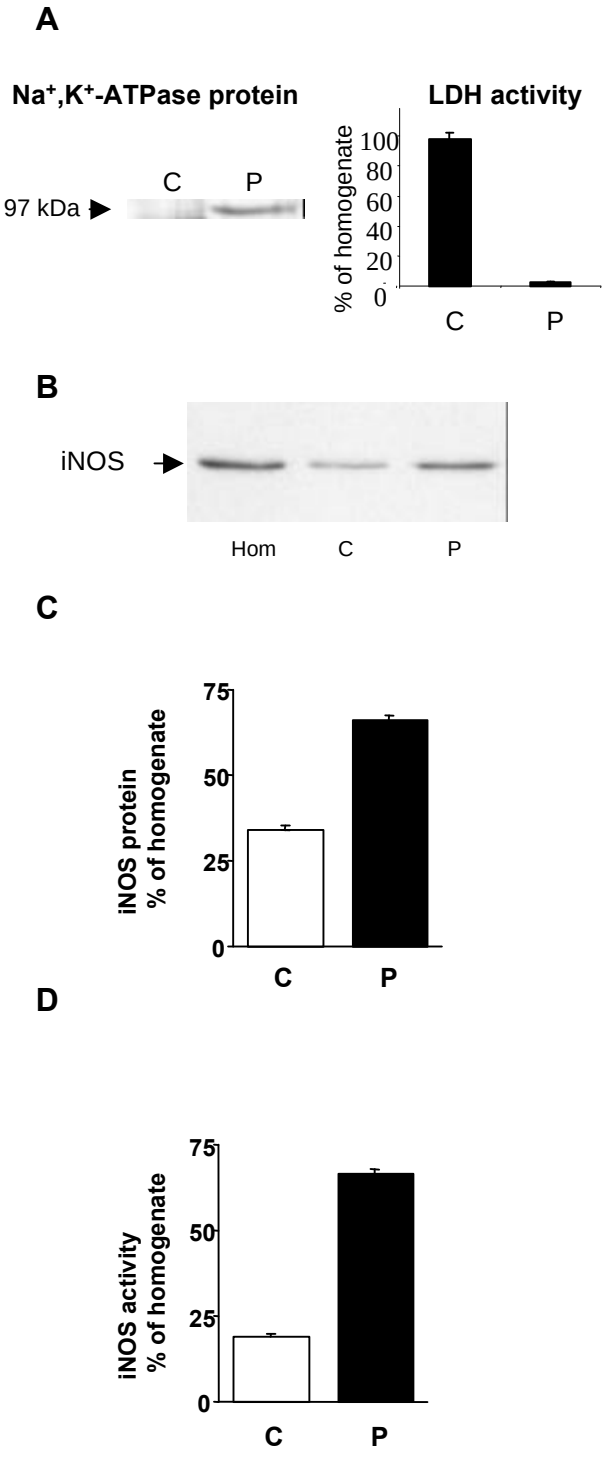

FIG. 1.

Hal-Inserm Author manuscript

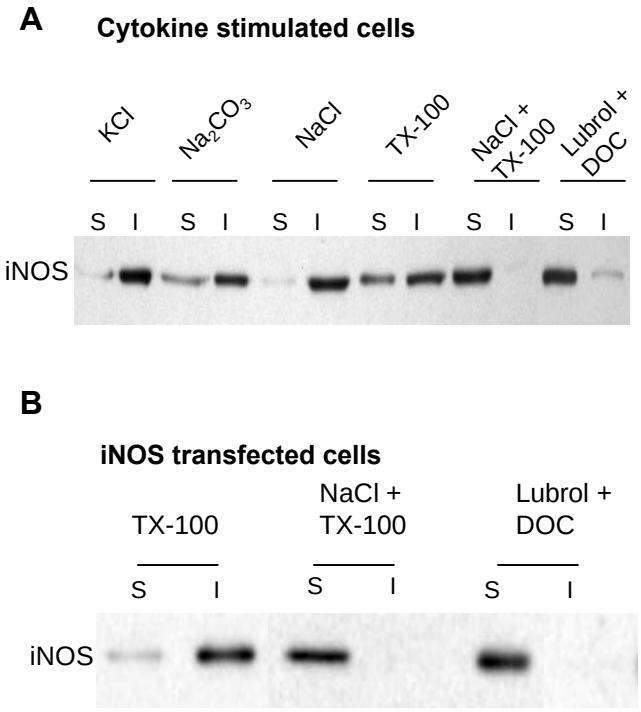

FIG. 2.

Hal-Inserm Author manuscript

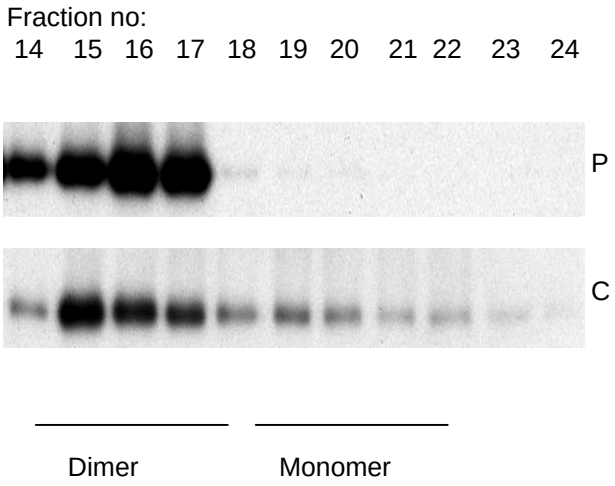

FIG. 3.

Hal-Inserm Author manuscript

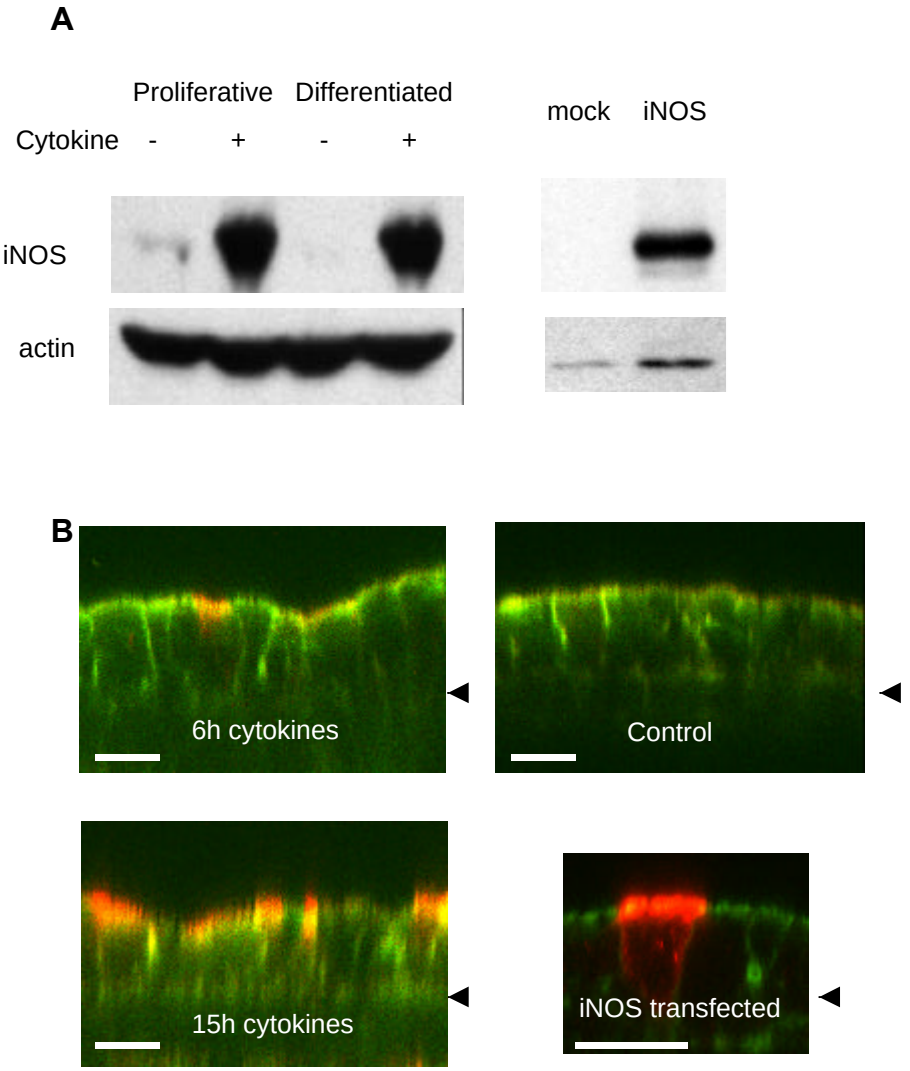

FIG. 4.

Hal-Inserm Author manuscript

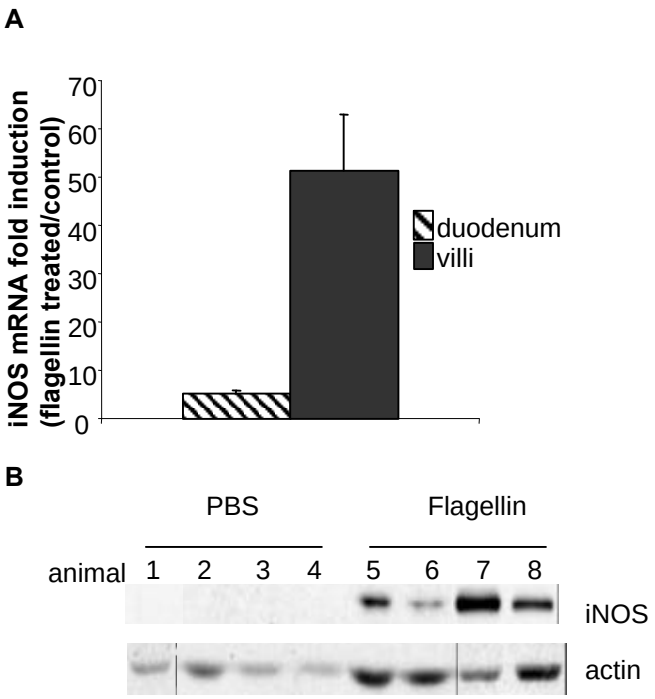

FIG. 5.

Hal-Inserm Author manuscript

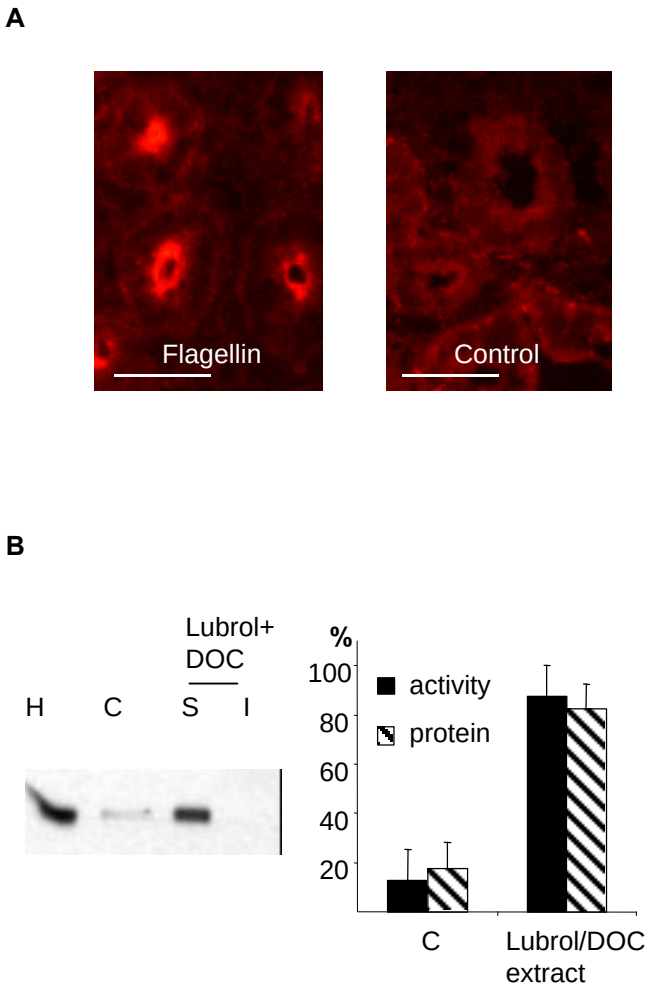

FIG. 6.